

UNCLASSIFIED

AD 268 138

*Reproduced
by the*

**ARMED SERVICES TECHNICAL INFORMATION AGENCY
ARLINGTON HALL STATION
ARLINGTON 12, VIRGINIA**



UNCLASSIFIED

NOTICE: When government or other drawings, specifications or other data are used for any purpose other than in connection with a definitely related government procurement operation, the U. S. Government thereby incurs no responsibility, nor any obligation whatsoever; and the fact that the Government may have formulated, furnished, or in any way supplied the said drawings, specifications, or other data is not to be regarded by implication or otherwise as in any manner licensing the holder or any other person or corporation, or conveying any rights or permission to manufacture, use or sell any patented invention that may in any way be related thereto.

62-1-5 NOX

NASA TN D-992

NASA TM D-992

ASTIA

BY

AS AD NO.

268 138

268138



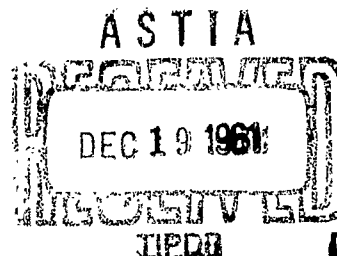
TECHNICAL NOTE

D-992

STUDY OF FLOW OVER OSCILLATING AIRFOIL MODELS
AT A MACH NUMBER OF 7.0 IN HELIUM

By Ali Arman

Langley Research Center
Langley Air Force Base, Va.



NATIONAL AERONAUTICS AND SPACE ADMINISTRATION
WASHINGTON

December 1961

NATIONAL AERONAUTICS AND SPACE ADMINISTRATION

TECHNICAL NOTE D-992

STUDY OF FLOW OVER OSCILLATING AIRFOIL MODELS

AT A MACH NUMBER OF 7.0 IN HELIUM

By Ali Arman

SUMMARY

A wind-tunnel study of unsteady flow at a Mach number of 7 in helium has been conducted on several sting-mounted wedge, double-wedge, and flat-plate airfoil models with three different leading-edge radii. The data were obtained by taking high-speed schlieren motion pictures of the decaying motion of the model as it was released from an initial deflection.

The shock-wave position observed on the sharp-leading-edge models during the oscillation was compared with that obtained by use of unsteady-flow theory as well as steady-state theory. Comparison of theoretical results indicated that no unsteady-flow effects exist over the range of reduced frequencies k , $0.007 \leq k \leq 0.030$, studied experimentally. The experimental results confirmed this finding as no unsteady-flow effects were detected in this reduced-frequency range. Comparison of shock-wave positions measured for the blunt models with those calculated by steady-state methods indicated fair agreement.

INTRODUCTION

In spite of the large quantity of steady-hypersonic-flow data which have been acquired in recent years, almost no information is available on unsteady- or oscillatory-hypersonic-flow phenomena. Unsteady-flow effects are of concern with regard to flutter and dynamic stability at hypersonic speeds. Most hypersonic unsteady-flow data have been obtained indirectly through flutter tests (for example, refs. 1 to 4). Some authors, such as those of references 5 to 8, have attempted to treat the problem analytically but their works have lacked experimental verification. In one of these papers (ref. 7) a method was developed by which the shock-wave position of an oscillating, sharp-leading-edge airfoil could be computed. The present study was designed to give experimental verification of this theory and to determine the applicability of quasi-steady flow theory. The effects of oscillations on the shock-wave position of a blunt airfoil were also investigated and compared with those obtained by use of the steady-state, zero-angle-of-attack method of reference 9.

Schlieren motion pictures were made of a series of simple models oscillating in helium at a Mach number of 7. The models studied were wedge and double-wedge sharp-leading-edge airfoils as well as airfoils with cylindrical leading edges of various radii. The reduced-frequency k range covered by the tests was $0.007 \leq k \leq 0.030$.

SYMBOLS

b	semichord, ft	L
D	diameter of cylindrical-leading-edge airfoil, in.	8
$\frac{x, y}{D}, \frac{y}{D}$	nondimensional rectangular coordinates attached to center of cylindrical leading edge of airfoil	3
k	reduced frequency, $b\omega/V$	9
q	dynamic pressure, lb/sq ft	
T	period of one cycle of oscillation, $2\pi/\omega$, sec	
V	free-stream velocity, ft/sec	
α	deflection angle, deg or radians	
δ	semiwedge angle, deg	
θ	angle between shock wave and free-stream velocity vector, deg or radians	
ρ	density, slugs/cu ft	
τ	thickness, percent chord	
ω	circular frequency, radians/sec	
t	time, sec	
f	model frequency, cps	

Subscripts:

r	theory of reference 7
s	steady-state theory

APPARATUS AND PROCEDURE

Wind Tunnel

This investigation was conducted in the 8-inch-diameter test section of the Langley hypersonic aeroelasticity tunnel which is an ambient-temperature tunnel using helium as a test medium. This tunnel is of the blowdown type; the test section used had a Mach number of 7 and a maximum dynamic-pressure capability of 5,000 pounds per square foot. A more detailed description of this facility is given in reference 1.

Schlieren System

A conventional single-pass schlieren system was used, which consisted of two 12-inch-diameter, 6-foot-focal-length mirrors. The light source was a mercury vapor lamp contained in an air-cooled case. A high-speed camera recorded the motion at approximately 3,000 frames per second. The adaptation of the schlieren system for this particular study is discussed subsequently.

Models

The models used for this study had wedge, double-wedge, and flat-plate airfoil sections, sketches of which are shown in figure 1. All models had an insert constructed of 1/8-inch-thick 17-7 PH stainless steel with an integral shaft for mounting to the sting support. Some of the models were lightened by drilling holes in the steel insert. A balsa overlay was used to produce the basic shape of the models. For the thicker flat-plate models, different size dowels were used to give the desired leading edge. The wedge and double-wedge airfoils had a fiber-glass coating over the balsa. The pertinent dimensions of all the models are listed in table I and a photograph of typical models is presented as figure 2.

A sketch of the model sting support is shown in figure 3. This support was constructed of stainless steel and was rigidly attached to the tunnel wall so that the model was at zero angle of attack. The natural frequency of the model mounted on the support could be varied by adjusting the position on the model's shaft at which it was clamped to the support. A photograph of the wedge model mounted on the sting support is shown as figure 4.

A small notched plug, 1/4 inch in diameter, was threaded to the steel core of each model as shown in figures 2, 3, and 4. A wire, hooked over the notch in the plug, was used to give the model an

initial deflection. For the purpose of this study it is assumed that the plug located on the upper surface of the model does not disturb the flow on the lower side.

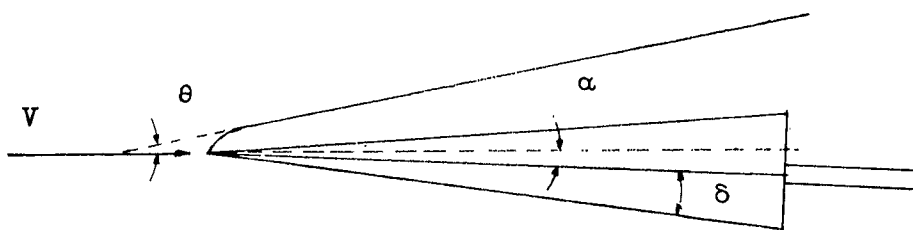
Tests

The procedure used for the tests was to quickly bring the tunnel test-section conditions to preselected values and then release the models and allow them to oscillate through a decaying motion at nearly constant test-section conditions. Oscillations were introduced by attaching a wire to the notched plug on the models and to the outside of the tunnel. The models were deflected to a predetermined angle by putting tension on the wire which was then cut to release the models at the proper time during each test. The wire hookup and the release of the models are shown in figure 5. It should be noted that the wire is carried downstream as soon as it is cut to release the models. High-speed schlieren motion pictures were taken of each test at approximately 3,000 frames per second.

Data Reduction

Although the schlieren system used in these tests is a conventional single-pass system, certain modifications were made for this particular study. A horizontal knife edge was used in order to obtain better sensitivity to the nearly horizontal shock waves. The characteristics of the schlieren system with the horizontal knife edge are such that the shock wave on the upper surface is white and the boundary layer is black, whereas on the bottom surface the boundary layer is white and the shock wave is black. In conventional systems the model appears as a black silhouette. In order to distinguish the model outline from the boundary layer, the upper half of the model side was painted white and the lower half was painted black (fig. 4); a spotlight was directed at the painted side of the model nearest the camera. Typical enlargements from the 16-millimeter motion pictures taken at intervals of about 0.2 of a period for a complete cycle of oscillation are shown in figure 5 for each of the three types of models. The effect of the front lighting can be seen by comparing figures 5(a) and 5(b) in which the models were illuminated with figure 5(c) in which the front lighting was not used.

From the 16-millimeter schlieren motion pictures 8-inch by 10-inch prints were made of the pertinent frames. The slope of the shock wave was obtained as shown in the following sketch; the pertinent angles were measured directly from the photographs:



As indicated in the sketch, the finite leading-edge radius and boundary-layer effects produce curvature of the shock at the leading edge. The shock angle measured was the angle between the downstream asymptote of the shock wave and the free-stream velocity vector.

RESULTS AND DISCUSSION

The test conditions including test-section density, velocity, dynamic pressure, model frequency, and the reduced frequency for each test are presented in table II.

The method of reference 7 gives the perturbation of the shock wave for small angles of attack about some mean angle. The theory was developed for simple harmonic motion and it was assumed that the reduced frequency was much less than 1. The method of reference 7 predicts a curved shock wave for the oscillating wedge, whereas steady-state theory indicates a straight line for the shock wave. However, at the frequencies of the present test the curvature terms in the theory of reference 7 are negligible. The theory also predicts the phase-angle lead or lag between the model oscillation and shock wave. The theoretical phase angles were very small for these tests and the examination of the experimental data has substantiated this result.

The actual response of the models was that of a decaying harmonic motion, rather than pure harmonic, with damping on the order of 1 percent critical. The small amount of damping allows the harmonic-motion theory to be applied over short periods of time.

A comparison of shock-wave angles calculated by steady-state theory with those calculated by the method of reference 7 is shown in figure 6 for the wedge model at $M = 7.0$ for flow deflection angles ranging from 3.5° to 11.5° and $k = 0.028$. The steady-state equations used in this comparison were obtained from reference 10. As can be seen, the two results are in close agreement.

The effect of frequency on the shock-wave angle is shown in figure 7. Both theory and experiment are shown for a constant amplitude

of oscillation, $\alpha = 2^\circ$, at various reduced frequencies of the wedge model. No effect of frequency is indicated by the unsteady-flow theory nor detected experimentally over the range of reduced frequencies covered by the study. In general, the measured change in the shock-wave angles is slightly less than the calculated change. It should be noted that, when the lines indicating the results of the unsteady-flow theory are extended to zero reduced frequency, they are tangent to the result obtained from steady-state theory.

Figure 8 illustrates the effect of oscillation amplitude on the shock-wave angle θ , with $k = 0.011$ to 0.028 . The two sets of data define the envelope of the shock angle on the lower surface of a typical model during a cycle of oscillation. Theory and experiment appear to be in good agreement for amplitudes up to at least 0.035 radian.

L
8
3
9

No unsteady-flow treatment is available for calculating the shock-wave position of blunt airfoils. However, the schlieren motion pictures indicated that the shock-wave shape was not only independent of frequency over the test range but oscillated in translation with no apparent pitching motion. The shock-wave shape was calculated by the steady-state, zero-angle-of-attack method of reference 9 by using a shock detachment angle of 36° which was obtained from some unpublished data obtained at the Langley Research Center. The shock shapes for the blunt-leading-edge models can be seen in figure 9. Although this theoretical method for determining shock shapes is more valid near the nose, fairly good agreement is obtained as far back as $\frac{1}{4}$ diameters. No detectable phase angles between the model motion and the shock-wave motion were observed over the test range for the blunt-leading-edge models.

CONCLUDING REMARKS

A wind-tunnel investigation of flow over oscillating airfoils has been conducted on several rectangular-planform models at a Mach number of 7. Schlieren motion pictures were taken during decaying oscillations of the models in pitch. Comparison of results obtained by use of unsteady-flow theory with those obtained by use of steady-state theory indicated that no unsteady-flow effects exist over the range of reduced frequencies k , $0.007 \leq k \leq 0.030$, studied experimentally. The experimental results confirmed this finding as no unsteady-flow effects were detected in this reduced-frequency range. The shock-detachment distance and shock-wave position on the blunt-leading-edge models could be calculated reasonably well by established steady-flow procedures within the frequency range of the tests.

Langley Research Center,
National Aeronautics and Space Administration,
Langley Air Force Base, Va., September 26, 1961.

REFERENCES

1. Morgan, Homer G., and Miller, Robert W.: Flutter Tests of Some Simpl Models at a Mach Number of 7.2 in Helium Flow. NASA MEMO 4-8-59L, 1959.
2. Miller, Robert W., and Hannah, Margery E.: Flutter Investigation of 60° to 80° Delta-Planform Surfaces at a Mach Number of 7.0. NASA TM X-325, 1960.
3. Gibson, Frederick W., and Mixson, John S.: Flutter Investigation at a Mach Number of 7.2 of Models of the Horizontal- and Vertical-Tail Surfaces of the X-15 Airplane. NASA MEMO 4-14-59L, 1959.
4. Lauten, William T., Jr., Levey, Gilbert M., and Armstrong, William O. Investigation of an All-Movable Control Surface at a Mach Number of 6.86 for Possible Flutter. NACA RM L58B27, 1958.
5. Hayes, Wallace D., and Probst, Ronald F.: Hypersonic Flow Theory. Academic Press, Inc., 1959, pp. 130-139.
6. Morgan, Homer G., Runyan, Harry L., and Huckel, Vera: Theoretical Considerations of Flutter at High Mach Numbers. Jour. Aero. Sci., vol. 25, no. 6, June 1958, pp. 371-381.
7. Sewell, Geoffrey L.: A Theory of Uniform Supersonic Flow Past a Thin Oscillating Aerofoil at Appreciable Incidence to the Main Stream. Aero. Quarterly, vol. V, pt. 3, Sept. 1954, pp. 185-194.
8. Sewell, Geoffrey L.: Theory of an Oscillating Supersonic Aerofoil. Aero. Quarterly, vol. II, pt. I, May 1950, pp. 34-38.
9. Love, Eugene S.: A Reexamination of the Use of Simple Concepts for Predicting the Shape and Location of Detached Shock Waves. NACA TN 4170, 1957.
10. Mueller, James N.: Equations, Tables, and Figures for Use in the Analysis of Helium Flow at Supersonic and Hypersonic Speeds. NACA TN 4063, 1957.

L
8
3
9

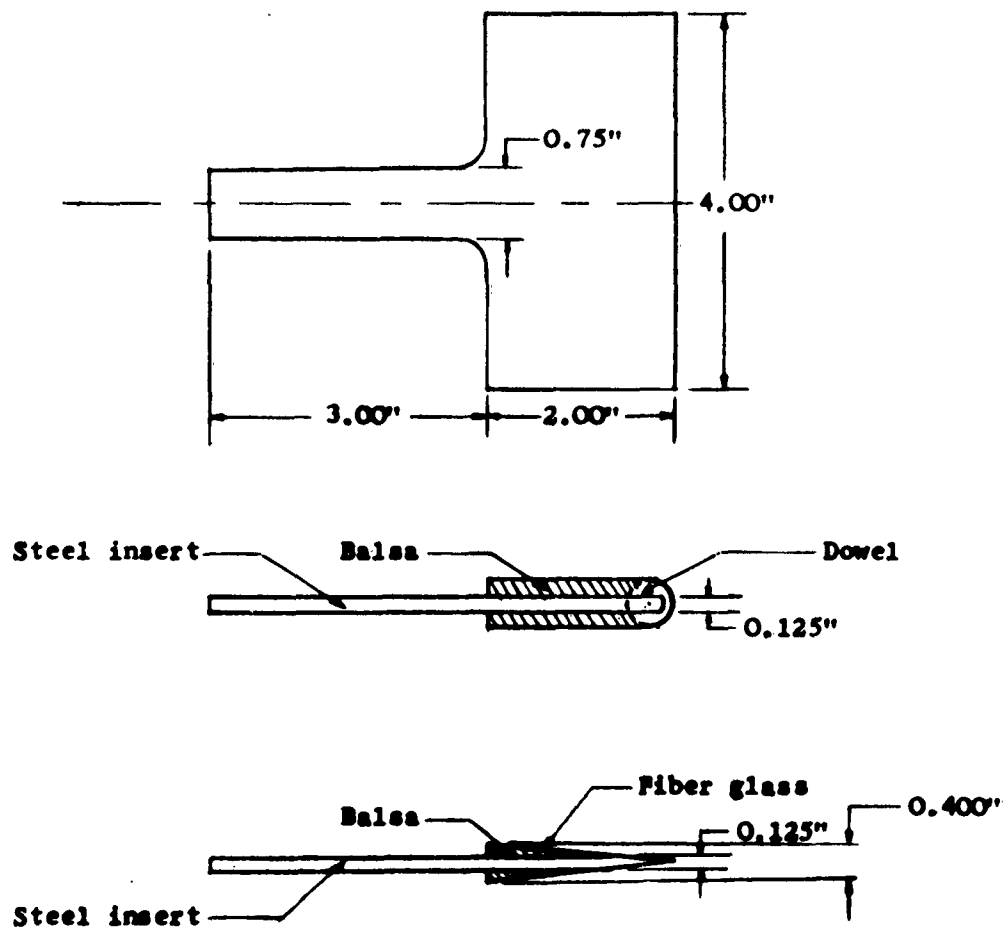
TABLE I.- TEST MODEL DATA

Airfoil section	Weight, g	Span, in.	Chord, in.	τ , percent chord	L.E. radius, in.
Wedge	87.60	4	2	20	0.002
Wedge	115.06	4	2	20	.002
Double wedge	240.36	4	4	10	.002
Double wedge	142.9	4	4	10	.002
Blunt leading edge	71.21	4	2	3.125	.0625
Blunt leading edge	78.86	4	2	6.25	.125
Blunt leading edge	86.51	4	2	10	.190

TABLE II.- TEST CONDITIONS

Airfoil section	Shaft length, in.	ρ , slugs/cu ft	V , ft/sec	q , lb/sq ft	f , cps	$b\omega/V$
Wedge	0.55	0.000112	5,754	1,851	311	0.028
	1.0	.000114	5,768	1,888	222	.020
	2.0	.000102	5,698	1,668	118	.011
Wedge	.65	.000111	5,761	1,844	268	.024
	1.0	.000106	5,768	1,760	201	.018
	2.0	.000120	5,747	1,973	110	.010
Double wedge	.55	.000122	5,677	1,969	94	.017
	1.0	.000106	5,684	1,796	70	.013
	2.0	.000112	5,698	1,941	38	.007
Double wedge	.55	.000106	5,698	1,736	112	.021
	1.0	.000106	5,684	1,717	86	.016
	2.0	.000117	5,677	1,881	46	.008
Blunt leading edge	.55	.000112	5,719	1,834	329	.030
	1.0	.000102	5,754	1,685	229	.021
	2.0	.000111	5,768	1,824	131	.012
Blunt leading edge	.55	.000117	5,754	1,933	298	.027
	1.0	.000097	5,845	1,656	217	.019
	2.0	.000112	5,705	1,814	123	.011
Blunt leading edge	.55	.000111	5,670	1,775	286	.026
	1.0	.000121	5,747	1,992	206	.019
	2.0	.000119	5,768	1,942	117	.011

L
8
3
9

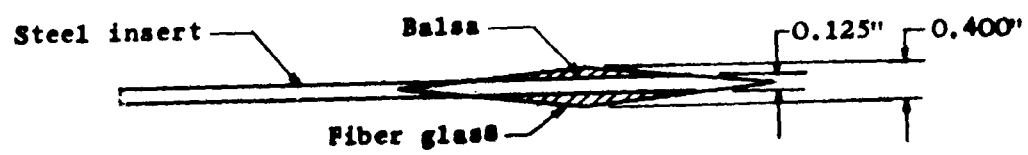
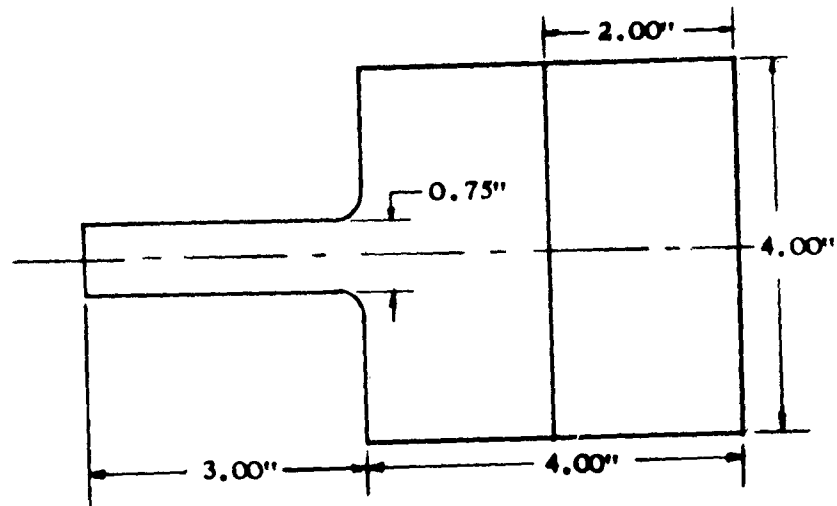


L-839

(a) Wedge and blunt-leading-edge models.

Figure 1.- Sketches of models.

L-839



(b) Double-wedge model.

Figure 1.- Concluded.

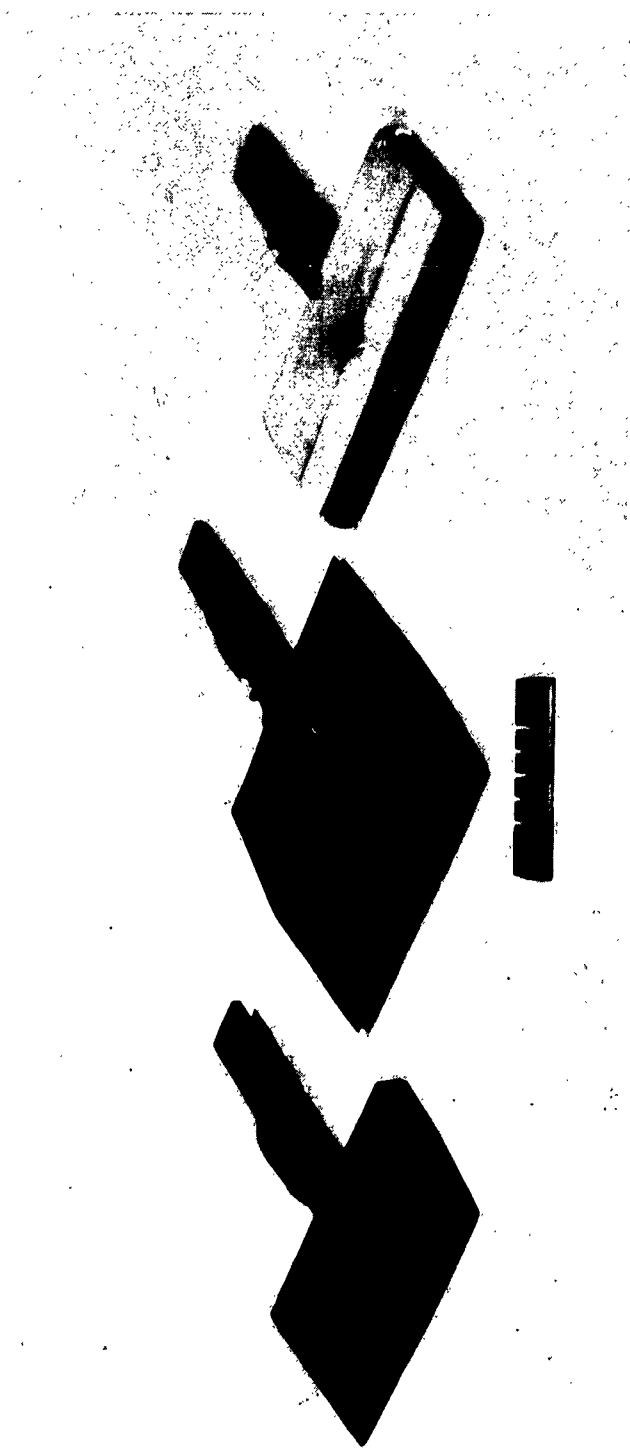


Figure 2.- Models used in the study. L-60-3828

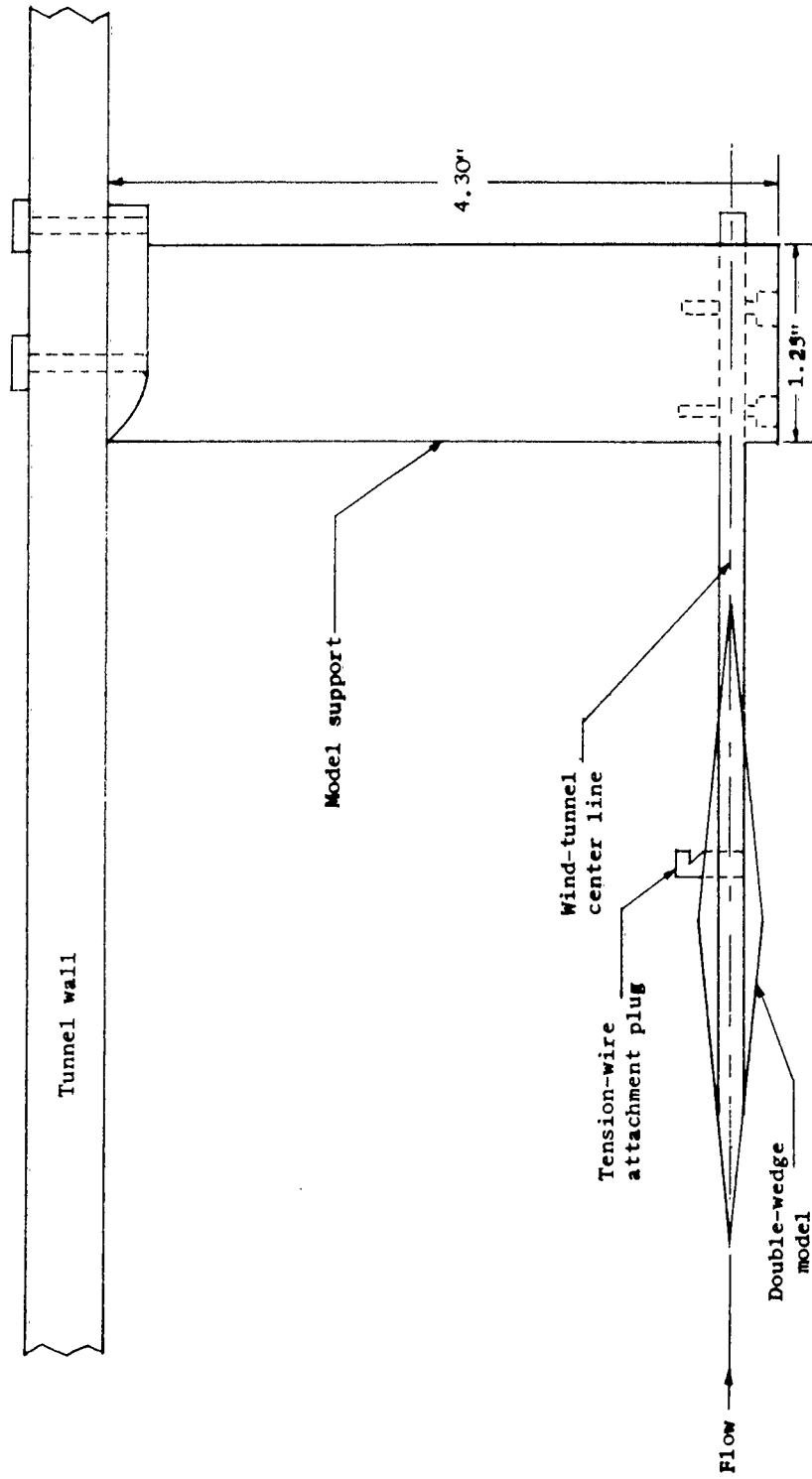
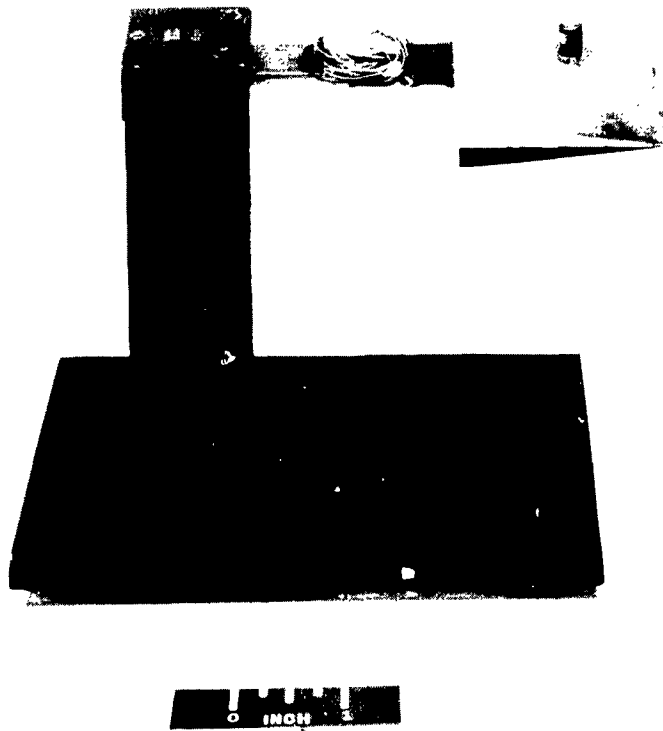


Figure 3.- Model sting support.



L-839

Figure 4.- Wedge-airfoil model mounted on support. L-60-3830

L-839



$t=0$



$t=0.2T$



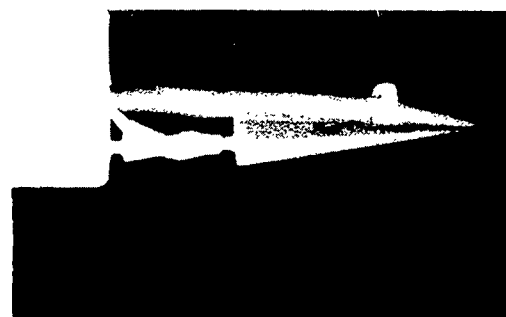
$t=0.4T$



$t=0.6T$



$t=0.8T$

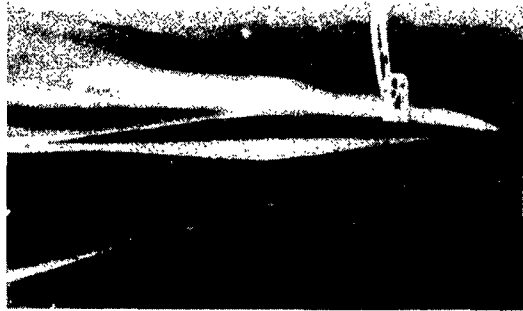


$t=T$

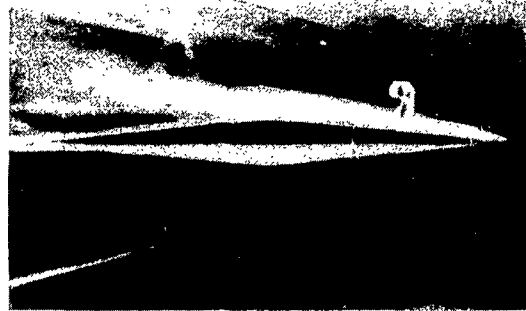
(a) Wedge model.

L-61-5105

Figure 5.- Schlieren photographs of airfoil models.



$t = 0$



$t = 0.2T$



$t = 0.4T$



$t = 0.6T$



$t = 0.8T$



$t = T$

(b) Double-wedge model.

L-61-5106

Figure 5.- Continued.

L-839

L-859



$t = 0$



$t = 0.2T$



$t = 0.4T$



$t = 0.6T$

$t = 0.8T$

$t = T$

(c) Blunt-leading-edge model.

L-61-5107

Figure 5.- Concluded.

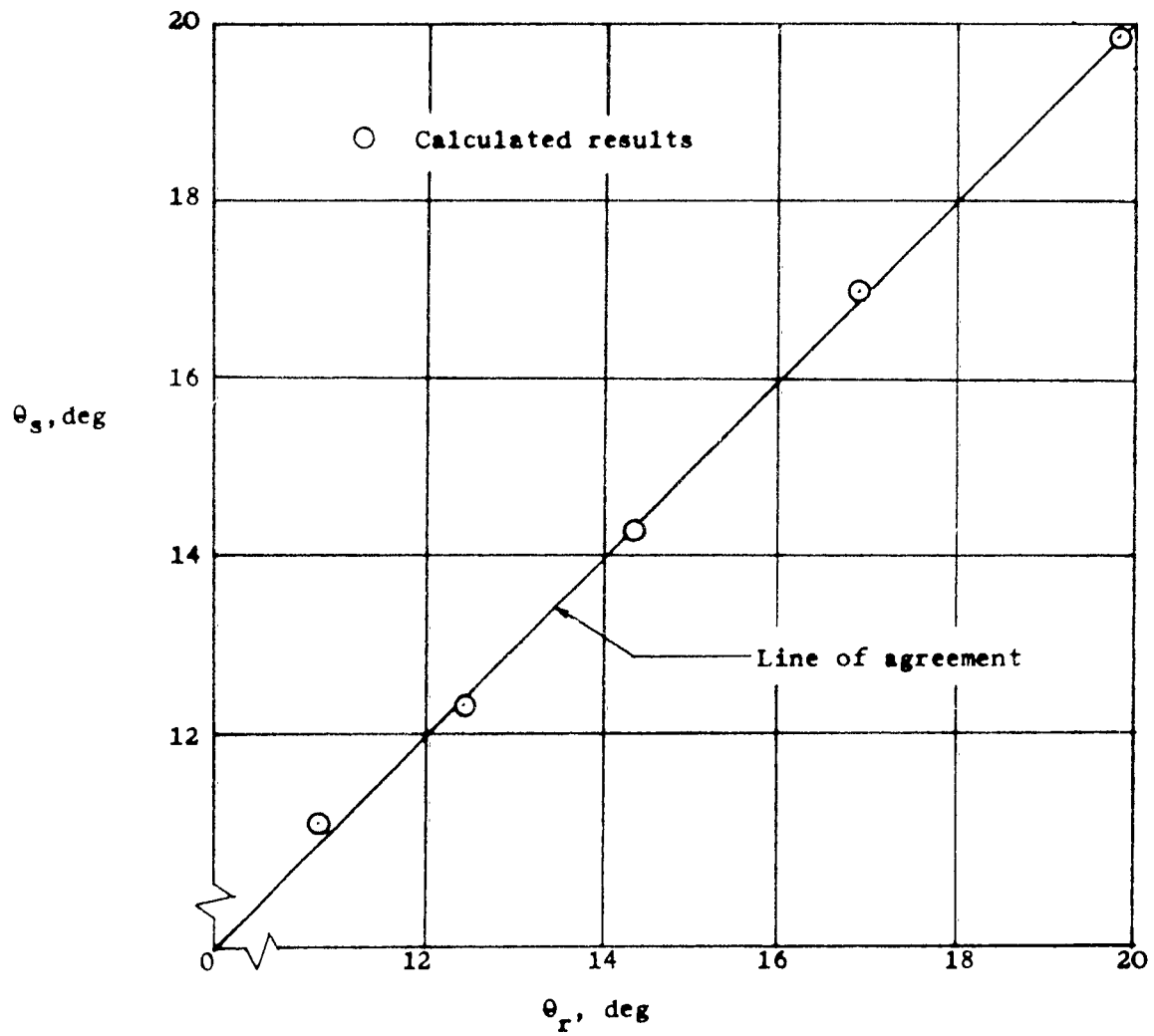


Figure 6.- Comparison of shock-wave angles calculated by steady-state theory and by the method of reference 7 for various flow deflection angles. $k = 0.028$.

L-839

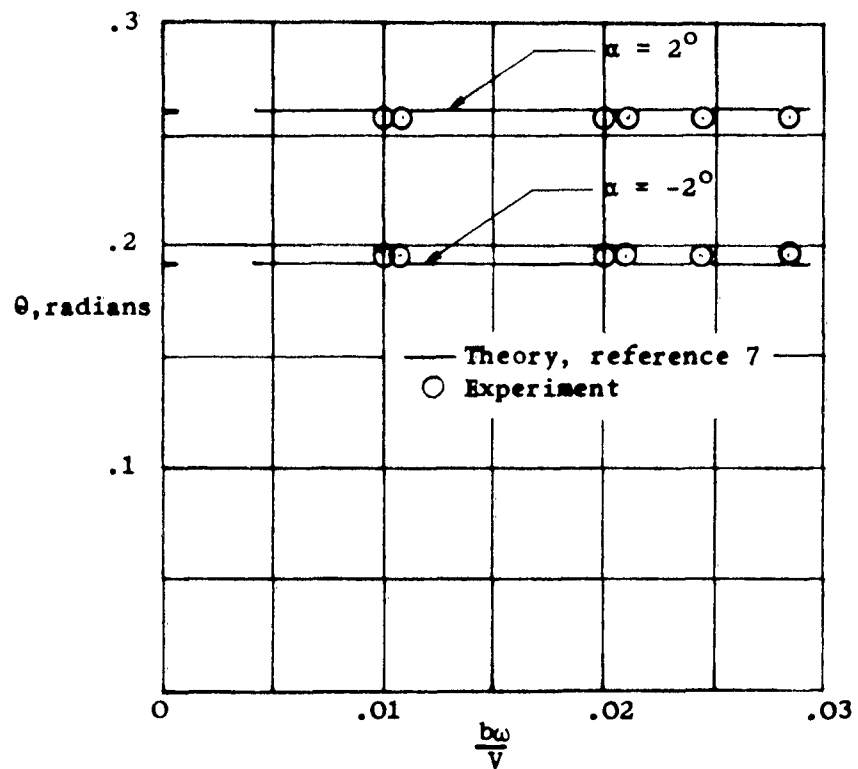


Figure 7.- Effect of reduced frequency on the shock-wave angle of the wedge models.

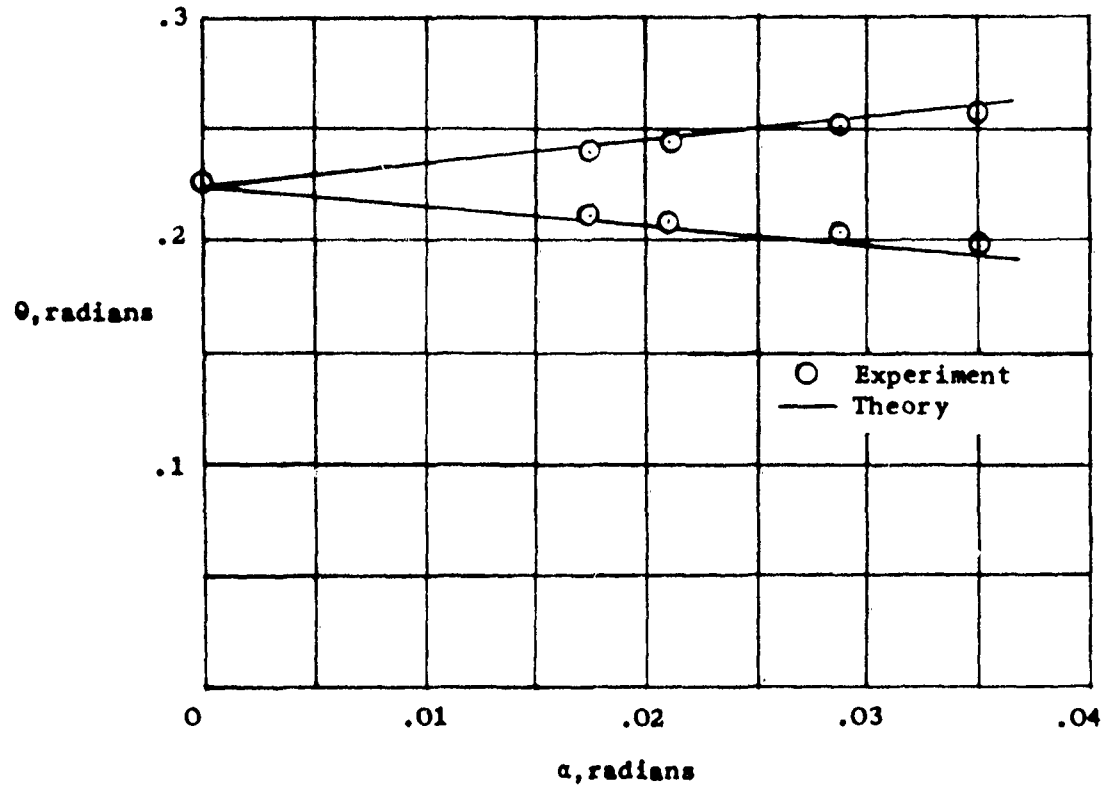


Figure 8.- Effect of oscillation amplitude on shock-wave angle θ .

L-839

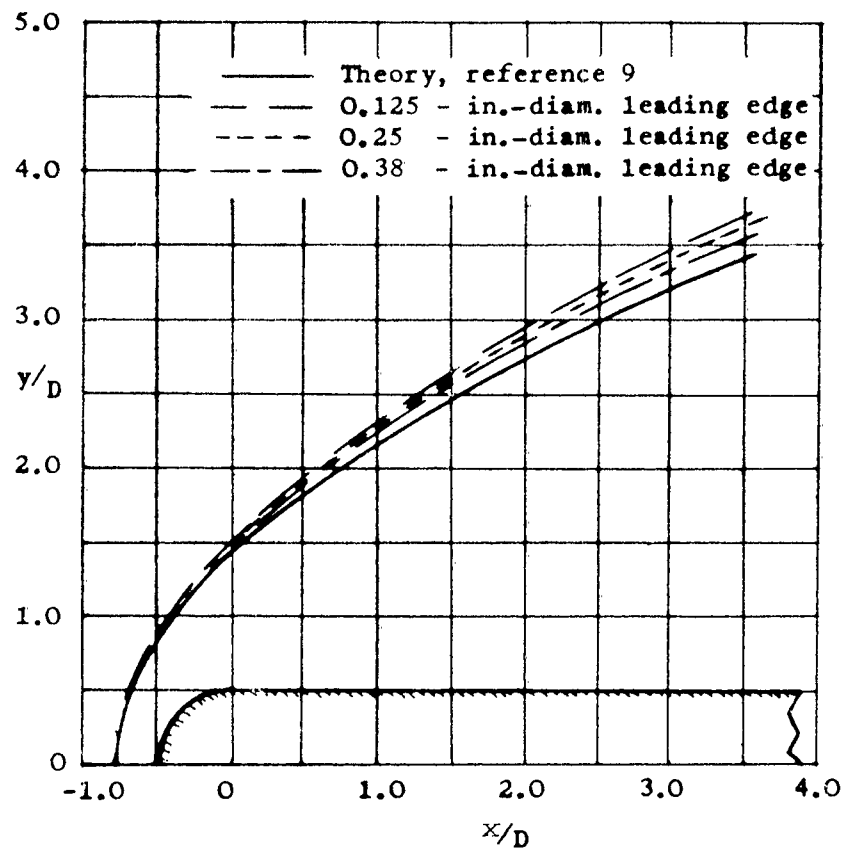


Figure 9.- Shock shape of oscillating blunt-leading-edge bodies.

